Intrinsic Character of the (3×3) to $(\sqrt{3} \times \sqrt{3})$ Phase Transition in Pb/Si(111)

I. Brihuega,[1] O. Custance,[1,*] Rubén Pérez,[2] and J. M. Gómez-Rodríguez[1,†]

[1]*Departamento Física de la Materia Condensada, Universidad Autónoma de Madrid, E-28049-Madrid, Spain*
[2]*Departamento Física Teórica de la Materia Condensada, Universidad Autónoma de Madrid, E-28049-Madrid, Spain*

We have investigated the (3×3) to $(\sqrt{3} \times \sqrt{3})$ reversible phase transition in Pb/Si(111) by means of variable temperature scanning tunneling microscopy and density functional first-principles calculations. By tracking exactly the same regions of the surface with atomic resolution in a temperature range between 40 and 200 K, we have observed the phase transition in real time. The ability to prepare and track exceptionally large domains without defects has allowed us to detect the intrinsic character of the phase transition at temperatures around 86 K. This intrinsic character is in full agreement with our first-principles calculations. Moreover, our results show that the hypothesis that point defects play a fundamental role as the driving force, reported for similar systems, can be discarded for Pb/Si(111).

Since the discovery of the (3×3) to $(\sqrt{3} \times \sqrt{3})R30°$ reversible phase transition in the $1/3$ monolayer (ML) systems of Pb or Sn on Ge(111) [1,2], a great number of experimental and theoretical works have been performed trying to understand its nature and driving force [3]. This phase transition consists on a lowering of the symmetry of the system produced by a change of the surface periodicity that evolves from a $(\sqrt{3} \times \sqrt{3})R30°$ ($\sqrt{3}$ in the following) at room temperature (RT) to a (3×3) at low temperature (LT). Various physical processes, such as a charge density wave due to electron-phonon coupling or electron-correlation effects [1,2,4], dynamical fluctuations stabilized by a soft phonon [5–7], interaction of defects with the (3×3) periodicity [8,9], or electron mediated adatom-adatom interaction [10], have been suggested to explain the different experimental results. Most of the works have been performed in the Sn/Ge(111) interface owing to the fact that this system can be more easily grown with a low density of defects, but even in this system, the surface is always present between 2% and 5% of the substitutional defects [9] that blur the intrinsic character of the phase transition.

The isovalent system Pb on Si(111) also presents the same temperature mediated phase transition [11,12], although it has not been the subject of such intensive studies. In this Letter we have investigated the $1/3$ ML phase of Pb/Si(111) in which we have been able to prepare extremely large domains (up to 20×20 nm^2) completely free of defects. These large free-of-defects regions, together with our ability to track the same area with atomic resolution in a wide temperature range because of our homebuilt drift-compensated scanning tunneling microscope, have allowed us to determine unambiguously the intrinsic character of the phase transition. We have found that the critical exponents in these large free-of-defects areas are consistent with the expected three-state Potts model [13,14], and a critical temperature $T_c = 86 \pm 2$ K has been obtained. Our first-principles density functional

calculations (DFT) show that the ground state at LT is the (3×3) symmetry with one of the three Pb atoms of the unit cell displaced upwards. We have also focused on the role played by the point defects. In the Pb/Si(111) system we do not observe any evidence of a defect-defect interaction with the (3×3) periodicity since the Si substitutional defects do not modify their positions when the temperature is varied between 40 and 200 K.

The experiments were carried out in an ultrahigh-vacuum system (base pressure below 5×10^{-11} Torr)
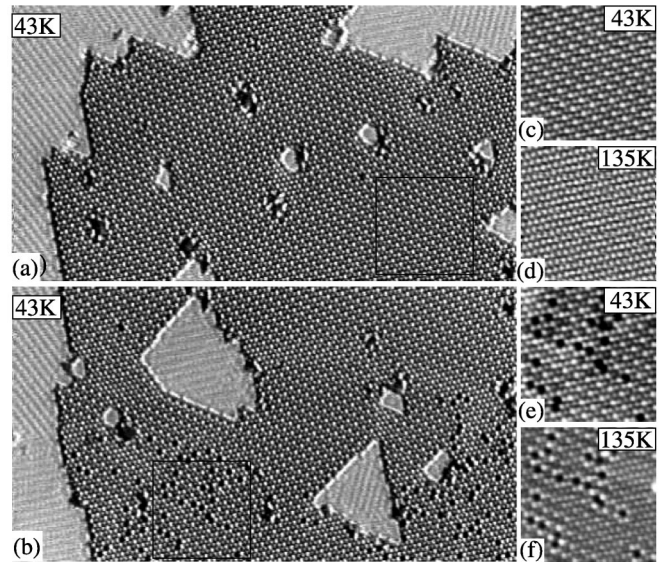

FIG. 1. (a),(b) STM images showing the general morphology of the sample at 43 K [the lower part of image (a) matches the upper part of image (b)]. (c),(d) The same free-of-defects area highlighted in (a) measured at 43 K and 135 K, respectively. (e),(f) The defective zoom-in region marked in (b) again at 43 K (e) and 135 K (f). Size of the images: 70×40 nm^2 [(a),(b)]; 13×13 nm^2 [(c)–(f)]. Sample bias, -1.5 V, and tunneling current, 0.1 nA, for all images. (a) and (b) are displayed in a derivative view [27].

equipped with a homebuilt variable temperature scanning tunneling microscope (VT-STM) which allows imaging at sample temperatures in the range of 40 to 400 K [12,15]. The sample preparation has already been described in Ref. [11]. Briefly it consists of depositing on clean recon-structed Si(111)-(7×7) surfaces ≈ 1 ML of Pb at RT followed by annealing at 450 °C for some minutes. The samples are then transferred to the VT-STM and slowly cooled down to temperatures as low as 40 K. This sample preparation procedure leads to the formation of surfaces presenting at LT a coexistence of ($\sqrt{7} \times \sqrt{3}$)-Pb islands with (3×3)-Pb domains [11,16]. The ($\sqrt{7} \times \sqrt{3}$)-Pb phase is stable up to temperatures of 250 K when it experiences a different phase transition [17,18].

Figure 1 shows typical STM images illustrating the general morphology of the samples prepared with the above described procedure. Together with ($\sqrt{7} \times \sqrt{3}$)-Pb islands, an extensive (3×3) single domain (70×40 nm^2) with large free-of-defects areas can be observed in 1(a), while smaller domains and defective regions with Si sub-stitutional atoms can be resolved in 1(b). Such sample morphology constitutes an ideal playground for the analy-sis of the phase transition and the influence on it of natural occurring defects. Figures 1(c) and 1(d) correspond to STM images measured exactly in the same zoom-in region highlighted in 1(a) at 43 K [1(c)] and 135 K [1(d)]. In this 13×13 nm^2 free-of-defects area we can see the existence of a (3×3) structure at 43 K [1(c)] and how the phase transition has already taken place at 135 K leading to a $\sqrt{3}$ reconstruction [1(d)]. Figures 1(e) and 1(f) correspond to the zoom-in region highlighted in a defective area in 1(b). Again, both images show exactly the same surface location at 43 and 135 K, respectively. In this defective area even at 135 K some patches of the (3×3) reconstruction can still be distinguished. These patches come from the local stabi-lization of the (3×3) structure due to the Si substitutional defects that are in this region.

Given our ability to track exactly the same surface region while varying the sample temperature, we have been able to follow the evolution of the phase transition in the real space and in real time for the first time. Figure 2 shows some frames extracted from an STM movie [19] measured continuously on the same sample spot while varying the temperature from 40 to 140 K. It corresponds to a region almost free of point defects (just one can be observed in the upper left part). As shown in Fig. 2(d) at 86 K most of the region has experienced a transition from a (3×3) symmetry to a $\sqrt{3}$ one. We have observed that this is the typical situation for our large free-of-defects domains.

The measurement and analysis of such a novel kind of STM movies [19] have allowed us to investigate the critical temperature for large and free-of-defects domains in great detail. Figure 3 shows a quantitative analysis performed on an STM movie measured in a 10×10 nm^2 area com-
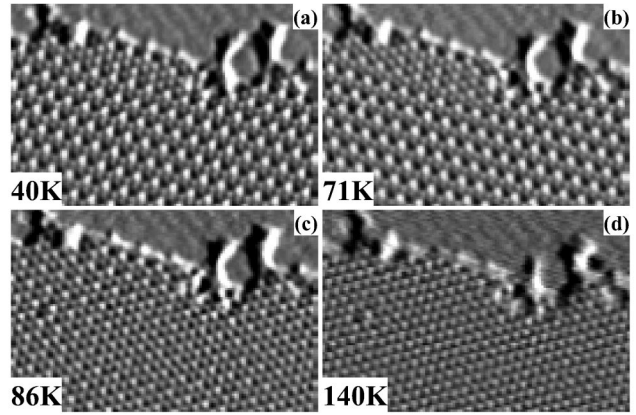

FIG. 2.   Constant current images extracted from an STM movie [19] spanning in temperature from 40 to 140 K. All the frames of the movie are measured in exactly the same region of the surface while the phase transition undergoes. Size of the images, 20×13 nm^2; sample bias, -1.5 V; tunneling current, 0.2 nA. The images are shown in a derivative mode [27].

pletely free of defects and spanning in temperature from 71 to 102 K. In order to do the analysis we have Fourier transformed each of the STM images in the movie. As a result, we have obtained a reciprocal space image which is reminiscent of a traditional low energy electron diffraction pattern (see insets of Fig. 3). As a critical parameter we have chosen the (3×3) peak intensity obtained from the addition of the contribution of the three nonequivalent (3×3) peaks, which we have plotted as a function of the temperature. Near T_c the (3×3) peak intensity (I) should
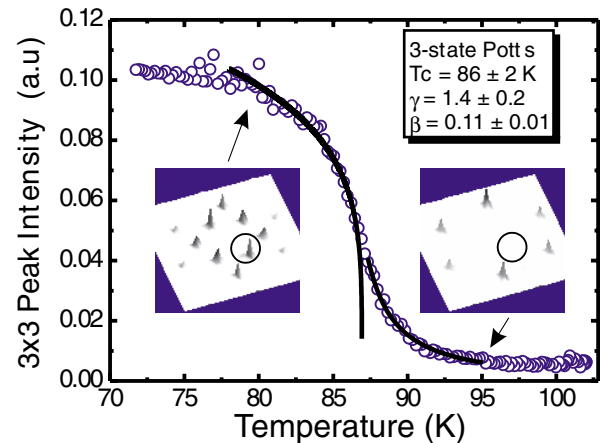

FIG. 3 (color online).   Plot of the (3×3) peak intensity as a function of the temperature. The intensity has been obtained from the Fourier transform (FT) of each of the frames of an STM movie measured in a 10×10 nm^2 free-of-defects area. The insets show 3D views of the typical FT below and above T_c [a circle outlines the position of one (3×3) peak]. The full lines correspond to a fit of the intensity obtained using $I \propto |t|^{\lambda}$, where, for $T < T_c$, $\lambda = 2\beta$ and, for $T > T_c$, $\lambda = -\gamma$. The experimental critical exponents are in very good agreement with the predicted three-state Potts model (see text).

scale according to a power law: $I \propto |t|^\lambda$, where $t = (T_c - T)/T_c$ is the reduced temperature. For $T < T_c$, $\lambda = 2\beta$ and for $T > T_c$, $\lambda = -\gamma$, where β and γ are the critical exponents associated with the order parameter and the susceptibility, respectively [20]. Using these expressions we were able to reproduce very precisely the evolution of the intensity near T_c. This evolution is absolutely reversible, and we obtain exactly the same results either increasing or decreasing the sample temperature [19]. From the experimental data fit we have obtained a transition temperature $T_c = 86 \pm 2$ K with critical exponents $\beta = 0.11 \pm 0.01$ for $T < T_c$, and $\gamma = 1.4 \pm 0.2$ for $T > T_c$. Because of the surface symmetry this phase transition is supposed to belong to the three-state Potts universality class, whose critical exponents β and γ are 0.11 and 1.44, respectively [13,14,20]. Thus, our experimental critical exponents are in very good agreement with the expected ones. It is important to stress that the value obtained for the transition temperature for these large free-of-defects regions is very reproducible within the experimental error.

Total energy plane-wave GGA(generalized gradient approximation)-DFT calculations [6,21] provide further evidence of the intrinsic character of the transition. We have performed an analysis [22] of the stability of the $\sqrt{3} \times \sqrt{3}$ structure with respect to the presence of a surface soft phonon with 3×3 periodicity, similar to the one developed for the isovalent Sn/Ge and Sn/Si(111) systems [6,7]. In this analysis, we start from a $\sqrt{3} \times \sqrt{3}$ structure (in a 3×3 unit cell), where the three Pb atoms are equivalent, we select one of them (Pb$_1$) and force it to move in the direction perpendicular to the surface. For each of these displacements, the other Pb atoms (Pb$_2$ and Pb$_3$) and all the semiconductor atoms are allowed to relax (up to the fifth layer) to their zero force positions under the constraint of the Pb$_1$ displacement. Figure 4(a) shows that the ground state corresponds to a (3×3) geometry with a Pb$_1$ displacement of ~ 0.2 Å and a height difference of 0.27 Å between the up and the down Pb atoms. Both the $\sqrt{3}$

structure and the (3×3) ground state in Pb/Si(111) are metallic, in good agreement with our experimental scanning tunneling spectroscopy (STS) measurements [see Figs. 4(b) and 4(c)] [23]. Our DFT calculations show that the presence of a surface soft phonon is associated with the phase transition in a similar way to that shown for the Sn/Ge(111) [6,7]. For the isovalent system Sn/Si(111) experimental evidence exists that this transition does not take place for temperatures down to 6 K [24], which is in agreement with DFT calculations that rule out the presence of a soft phonon in the Sn/Si(111) system [6].

We have also studied the influence of point defects in the phase transition. It has been reported that in the Sn/Ge(111) system point defects (Ge in substitutional positions) act as pinning centers of the phase transition originating an exponentially attenuated modulation with the (3×3) symmetry [8,9]. The inverse decay length of this damped modulation was found to be linear with temperature, and from its extrapolation to zero a transition temperature was proposed. Moreover, these authors also reported the existence of a defect-defect interaction with the (3×3) periodicity which forced the motion of the defects at LT and the alignment of them onto a honeycomb sublattice near the critical temperature. As shown above (Fig. 1), in the Pb/Si(111) system we have observed the coexistence of domains with large free-of-defects areas with domains presenting point defects that are mainly substitutional Si atoms [25]. In order to investigate a hypothetical motion of the defects due to a defect-defect interaction, we have tracked this kind of defective regions in a temperature range from 40 to 200 K. We have never detected any motion of substitutional point defects in any of these measurements. As an example, two STM images of exactly the same region measured at 40 and 200 K are shown in Fig. 5. None of the point defects present in this region modifies its position as the temperature is increased up to values far away from the transition temperature. Therefore, no evidence of a long-range defect-defect mediated interaction has been detected in the Pb/Si(111) system (if there is any interaction, it must be too weak to
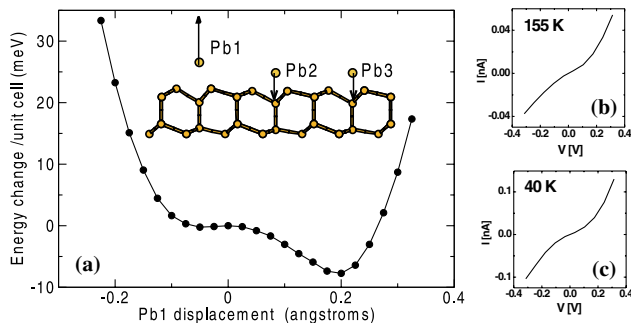

FIG. 4 (color online). (a) GGA-DFT total energy as a function of Pb$_1$ displacement perpendicular to the surface. The energy of the $\sqrt{3} \times \sqrt{3}$ structure is taken as the reference. (b),(c) Experimental STS average spectra above (b) and below (c) the phase transition.
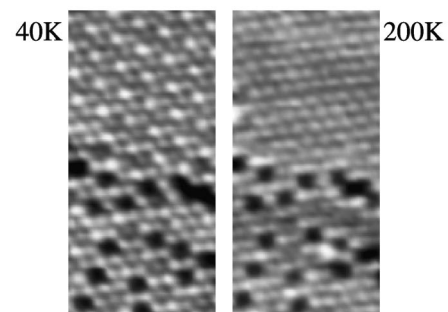

FIG. 5. STM images of the same defective region measured at 40 K (left) and 200 K (right). None of the point defects modifies its position as the temperature is increased. Size of the images, 6×13 nm^2; sample bias, -1.5 V; tunneling current, 0.1 nA.

induce a substitutional Si defect hopping) [26]. Moreover, although we have observed that Si substitutional defects may locally stabilize the LT (3×3) phase and thus increase the critical temperature for a defective area [Fig. 1(f)], very short decay lengths are detected with a less noticeable dependence with the sample temperature compared to the Sn/Ge(111) system [12]. All these observations reinforce the intrinsic character of the phase transition in Pb/Si(111) and discard the influence of substitutional point defects as the fundamental driving force.

In conclusion, we have studied the 1/3 ML Pb/Si(111) system in a temperature range from 40 to 200 K. We have been able to measure STM movies with atomic resolution tracking the same surface region over the whole temperature range. In these STM movies the (3×3) to $\sqrt{3}$ reversible phase transition has been observed for the first time in the real space in real time. In our system the surface is composed of large free-of-defects areas coexisting with more defective regions. Because of this particular morphology, we have been able to study independently the phase transition in the large free-of-defects areas and the role played by point defects. A transition temperature of 86 K has been obtained and the critical exponents have been found to be in very good agreement with the ones associated with a three-state Potts universality class. Although the point defects locally stabilize the (3×3) reconstruction, they should be discarded as the fundamental driving force for the phase transition. Our experiments provide strong evidence that a hypothetical long-range interaction between defects is too weak to induce a rearrangement of them at low temperature. Moreover, DFT calculations show the presence of a surface soft phonon in the 1/3 ML Pb/Si(111) that leads to a ground state with a (3×3) configuration at LT. All these experimental and theoretical results demonstrate the intrinsic character of this phase transition.

*Present address: Handai Frontier Research Center (FRC), 2-1 Yamada-Oka, Suita, 565-0871, Osaka, Japan.
†Corresponding author.
Electronic address: josem.gomez@uam.es

[1] J. M. Carpinelli *et al.*, Nature (London) **381**, 398 (1996).
[2] J. M. Carpinelli *et al.*, Phys. Rev. Lett. **79**, 2859 (1997).
[3] J. Ortega, R. Pérez, and F. Flores, J. Phys. Condens. Matter **14**, 5979 (2002); L. Petersen, Ismail, and E. W. Plummer, Prog. Surf. Sci. **71**, 1 (2002), and references therein.
[4] A. Goldoni and S. Modesti, Phys. Rev. Lett. **79**, 3266 (1997).
[5] J. Ávila *et al.*, Phys. Rev. Lett. **82**, 442 (1999).
[6] R. Pérez, J. Ortega, and F. Flores, Phys. Rev. Lett. **86**, 4891 (2001).
[7] D. Farías *et al.*, Phys. Rev. Lett. **91**, 016103 (2003).
[8] A. V. Melechko *et al.*, Phys. Rev. Lett. **83**, 999 (1999).
[9] A. V. Melechko *et al.*, Phys. Rev. B **61**, 2235 (2000).
[10] J. R. Shi *et al.*, Phys. Rev. Lett. **91**, 076103 (2003).
[11] O. Custance *et al.*, Surf. Sci. **482–485**, 1399 (2001).
[12] O. Custance, Ph.D. thesis, Universidad Autónoma de Madrid, 2002.
[13] L. Floreano *et al.*, Phys. Rev. B **64**, 075405 (2001).
[14] R. J. Baxter, *Exactly Solvable Models in Statistical Mechanics* (Academic Press, London, 1982).
[15] O. Custance *et al.*, Phys. Rev. B **67**, 235410 (2003).
[16] S. Brochard *et al.*, Phys. Rev. B **66**, 205403 (2002).
[17] K. Horikoshi *et al.*, Phys. Rev. B **60**, 13 287 (1999).
[18] J. Slezák, P. Mutombo, and V. Cháb, Phys. Rev. B **60**, 13 328 (1999).
[19] See EPAPS Document No. E-PRLTAO-94-018507 for STM movies from which images are extracted for measurement analysis. A direct link to this document may be found in the online article's HTML reference section. The document may also be reached via the EPAPS homepage (http://www.aip.org/pubservs/epaps.html) or from ftp.aip.org in the directory /epaps/. See the EPAPS homepage for more information.
[20] G. C. Wang and T. M. Lu, Phys. Rev. B **31**, 5918 (1985).
[21] CASTEP 4.2 Academic version, licensed under the UKCP-MSI Agreement, 1999. M. C. Payne *et al.*, Rev. Mod. Phys. **64**, 1045 (1992).
[22] We use a (3×3) unit cell with three Pb atoms and six Si layers, the last one being saturated with H atoms. Ultrasoft pseudopotentials (including d Pb orbitals as valence states) and a cutoff of 260 eV have been used.
[23] Both the $\sqrt{3}$ structure and the (3×3) ground state in Pb/Si(111) are metallic, in good agreement with our experimental STS measurements. A detailed analysis of these STS measurements will be published elsewhere.
[24] H. Morikawa, I. Matsuda, and S. Hasegawa, Phys. Rev. B **65**, 201308(R) (2002).
[25] J. M. Gómez-Rodríguez, J. Y. Veuillen, and R. C. Cinti, Surf. Sci. **377–379**, 45 (1997).
[26] Some short-range order exists in the different mosaic phase (50% Si) at RT that indicates an effective nearest-neighbor repulsion between Si adatoms [see E. Ganz *et al.*, Phys. Rev. B **43**, 7316 (1991); L. Ottaviano *et al.*, Phys. Rev. B **67**, 045401 (2003)]. This short-range interaction should not be confused with the long-range (3×3) interaction discarded by the present experiments.
[27] When we have the coexistence of (3×3)-Pb domains with $(\sqrt{7} \times \sqrt{3})$-Pb islands on the same image, we present it in a derivative view in order to visualize simultaneously both phases with atomic resolution.